

The response of Northern Hemisphere polar lows to climate change in a 25 km high-resolution global climate model

Article

Published Version

Creative Commons: Attribution 4.0 (CC-BY)

Open access

Bresson, H., Hodges, K. I. ORCID: <https://orcid.org/0000-0003-0894-229X>, Shaffrey, L. C. ORCID: <https://orcid.org/0000-0003-2696-752X>, Zappa, G. and Schiemann, R. ORCID: <https://orcid.org/0000-0003-3095-9856> (2022) The response of Northern Hemisphere polar lows to climate change in a 25 km high-resolution global climate model. *Journal of Geophysical Research: Atmospheres*, 127 (4). e2021JD035610. ISSN 2169-8996 doi: [10.1029/2021JD035610](https://doi.org/10.1029/2021JD035610) Available at <https://centaur.reading.ac.uk/97942/>

It is advisable to refer to the publisher's version if you intend to cite from the work. See [Guidance on citing](#).

To link to this article DOI: <http://dx.doi.org/10.1029/2021JD035610>

Publisher: American Geophysical Union

All outputs in CentAUR are protected by Intellectual Property Rights law, including copyright law. Copyright and IPR is retained by the creators or other copyright holders. Terms and conditions for use of this material are defined in

the [End User Agreement](#).

www.reading.ac.uk/centaur

CentAUR

Central Archive at the University of Reading

Reading's research outputs online



RESEARCH ARTICLE

10.1029/2021JD035610

Key Points:

- The present representation of Northern Hemisphere PLs in a high-resolution global climate model is found in agreement with previous studies
- The number of PLs is found to decrease by 60% by the end of the 21st century in the RCP8.5 scenario, but new PL locations emerge
- The decrease of PL activity in the future is attributed to an atmospheric static stability increase in a baroclinic instability reduction

Supporting Information:

Supporting Information may be found in the online version of this article.

Correspondence to:

H. Bresson,
h.bresson@reading.ac.uk

Citation:

Bresson, H., Hodges, K. I., Shaffrey, L. C., Zappa, G., & Schiemann, R. (2022). The response of Northern Hemisphere polar lows to climate change in a 25 km high-resolution global climate model. *Journal of Geophysical Research: Atmospheres*, 127, e2021JD035610. <https://doi.org/10.1029/2021JD035610>

Received 26 JUL 2021

Accepted 24 JAN 2022

The Response of Northern Hemisphere Polar Lows to Climate Change in a 25 km High-Resolution Global Climate Model

H. Bresson^{1,2} , K. I. Hodges³, L. C. Shaffrey³ , G. Zappa^{1,4}, and R. Schiemann³ 

¹Department of Meteorology, University of Reading, Reading, UK, ²Now at Laboratoire d'Optique Atmosphérique, CNRS UMR, University of Lille, Lille, France, ³National Centre for Atmospheric Science, University of Reading, Reading, UK, ⁴National Research Council of Italy, Institute of Atmospheric Sciences and Climate (CNR-ISAC), Bologna, Italy

Abstract Polar lows (PLs) are small, intense cyclones that form at high latitudes during the winter. Their high wind speeds and heavy precipitation can have substantial impacts on shipping, coastal communities and infrastructure. However, low-resolution climate models poorly simulate PLs, which reduces the confidence in their future projections. In this study, Northern Hemisphere (NH) PLs are assessed for the first time in a high-resolution (25 km) global atmosphere-only climate model, N512 HadGEM3-GA3, for both present-day and future RCP8.5 climate scenarios. The representation of PLs is found to agree reasonably well with the NCEP-CFS reanalysis. The number of NH PLs are projected to substantially decrease (by over 60%) by the end of the 21st century, which is largely due to an increase in atmospheric static stability. Large decreases in PL activity are found in the Norwegian Sea, north-east Atlantic and north-west Pacific Oceans. Smaller changes are found in regions of current PL activity, such as the Barents and Labrador Seas, while new regions of PL activity along the northern Russian coastline are found where the Arctic sea ice is projected to disappear. The spatial differences found in future PL activity could have a substantial impact on human activity in the Arctic region.

Plain Language Summary Polar lows (PLs) are small but intense storms that form during winter at high latitudes and affect regions such as Scandinavia, Northern Russia and Japan. Because of their strong winds and precipitation, PLs can cause damage to infrastructure, shipping and coastal communities. In this study, PLs are assessed for the first time in a high-resolution (25 km) global climate model for both present climate conditions and a future climate scenario in the Northern Hemisphere. The number of PLs is found to substantially decrease by the end of the 21st century, mainly due to a reduction in vertical temperature differences in the atmosphere. However, new regions of PL activity are found over the Arctic Ocean where the sea ice is projected to retreat.

1. Introduction

Polar lows (PLs) are small (typically 200–500 km in diameter with a maximum of 1,000 km) intense cyclonic systems that occur at high latitudes. PLs are short-lived, present strong wind speeds and are often associated with poor visibility, high precipitation and large ocean waves (Rasmussen and Turner (2003), page 13; Orimolade et al. (2016); Orimolade et al. (2017)). Consequently, PLs can cause substantial damage to shipping, offshore infrastructure and coastal communities (Jung et al., 2016; West & Hovelsrud, 2010). PLs consist of a range of polar mesoscale systems, which have been described to span from predominantly convective and hurricane-like systems (similar to their tropical counterparts though smaller in size, (Emanuel and Rotunno (1989); Rasmussen and Turner (2003), page 13) to primarily baroclinic systems (Mansfield, 1974). “Hybrid” systems (Bracegirdle & Gray, 2008), where both baroclinic instability and convective mechanisms play a role, are also observed. A series of dynamical pathways and conceptual models has been proposed for PL development including moist baroclinic instability (Harrold & Browning, 1969; Terpstra et al., 2015), surface thermal instability (Radovan et al., 2019), frontal instability (Claud et al., 2004; Føre et al., 2011), air-sea interaction through the Convective Instability of the Second Kind (CISK) and Wind-induced Surface Heat Exchange (WISHE) theory (Emanuel & Rotunno, 1989; Gray & Craig, 1998; Rasmussen, 1979). However, aiming to explain the development of PLs, those models are based on particular assumptions, which may not fully reflect the complexity of PLs development. Recent studies have challenged the idea that an hurricane-like convective-driven intensification really takes place, and proposed that baroclinic instability is the main actor in PLs activity, and always play the dominant role in fueling their development and in shaping their spatial structure (Stoll et al., 2021; Terpstra et al., 2021;

© 2022. The Authors.

This is an open access article under the terms of the [Creative Commons Attribution License](#), which permits use, distribution and reproduction in any medium, provided the original work is properly cited.

Terpstra & Watanabe, 2020). Indeed some case studies looking at hurricane-like PLs found no strong evidence of hurricane-like intensification mechanism (Føre et al., 2012; Kolstad et al., 2016).

Despite the multitude of theories about PL development, the limitation of the observational network and the insufficient resolution of reanalysis data means considerable uncertainty remains so that no theory fully explains all the types of PL activity and more case study and climatology of PLs must continue to help us improve our knowledge. Hence, as the broad range of PL types makes it difficult to assess a priori how PLs might respond to climate change, and any information on their future response has to be gained via simulations with climate models. In addition, the small spatial scale of PLs means that they are often poorly represented in the coarse resolution climate models.

The study of Zahn and von Storch (2010) investigated PLs in dynamically downscaled regional climate model simulations over the North Atlantic (NA) and Nordic Seas driven by historical and future climate simulations from the CMIP3 models. They found a decrease of 53% in PL numbers at the end of the 21st century compared to the present day. This decrease affected both weak and intense PLs and was shown to be closely associated with a projected increase in atmospheric static stability. This increase in atmospheric static stability was also found in Mallet et al. (2017) and was shown to be due to a faster increase of the mid-tropospheric temperature compared to the Sea Surface Temperature (SST) over the NA and the Nordic Seas. The relatively slow warming of SST is affected by the slowdown of the Atlantic Meridional Overturning Circulation (AMOC, Woollings et al. (2012); Gervais et al. (2018)). These changes in the large-scale winter environment were also found to be associated with a reduction in the number of Cold Air Outbreaks (CAO) over the Arctic region (Kolstad & Bracegirdle, 2008), linked to the projected decrease in sea ice (Papritz et al., 2019). A similar reduction in the projected changes in PLs (by the end of the 21st century in response to the RCP8.5 emissions scenario) over the NA and Nordic Seas has been found in other studies using a statistical-dynamical method that creates synthetic storms (Romero & Emanuel, 2017) and with the HARMONIE regional climate model downscaled from the CESM (Community Earth System Model) global climate model (Landgren et al., 2019). In these studies PL numbers were found to decline over the NA and the Nordic Seas by 10%–15% and 5%–20% respectively. The differences in projected mean PL numbers between Zahn and von Storch (2010), Romero and Emanuel (2017) and Landgren et al. (2019) are relatively large, highlighting the need for further investigation.

Previous studies have been performed with regional climate models, statistical-dynamical methods and/or relatively low horizontal resolution climate models in which PLs may not be well represented. To overcome these potential limitations, this study explores for the first time the response of PLs to climate change using high-resolution global climate model simulations, which have previously been shown to be of sufficient horizontal resolution to capture Mediterranean mesoscale cyclones similar to PLs (Tous et al., 2016), as well as mesoscale Tibetan Plateau Vortices (TPV, Curio et al. (2018); Curio et al. (2019)). Using a high-resolution global climate model allows the investigation of the global response of PLs to climate change, as well as the investigation of PL characteristics, such as associated wind speed maxima, and their interaction with the large-scale changes in atmospheric circulation. Specifically, the research questions addressed by this paper are:

1. How well are present-day PLs represented in a 25 km high-resolution global climate model?
2. How are PLs projected to respond to climate change?
3. How does the large-scale environment influence future changes in PLs?

Section 2 describes the data and the PL tracking scheme. The present-day representation of PLs in the climate model is evaluated using reanalysis in Section 3. The response of PLs to climate change, as well as the influence of the large-scale environment, are then examined in Section 4. Finally, conclusions and future work are discussed in Section 5.

2. Data and Methodology

2.1. Data

The data used in this study are from the UK on PRACE weather-resolving Simulations of Climate for global Environmental risk (UPSCALE) high-resolution simulations (Mizielinski et al., 2014). The UPSCALE data set is a series of ensemble simulations based on the Hadley Centre Global Environment Model version 3 Global Atmosphere-only version 3 (HadGEM3-GA3) model (Williams et al., 2015). For this study, the 6-hourly data of

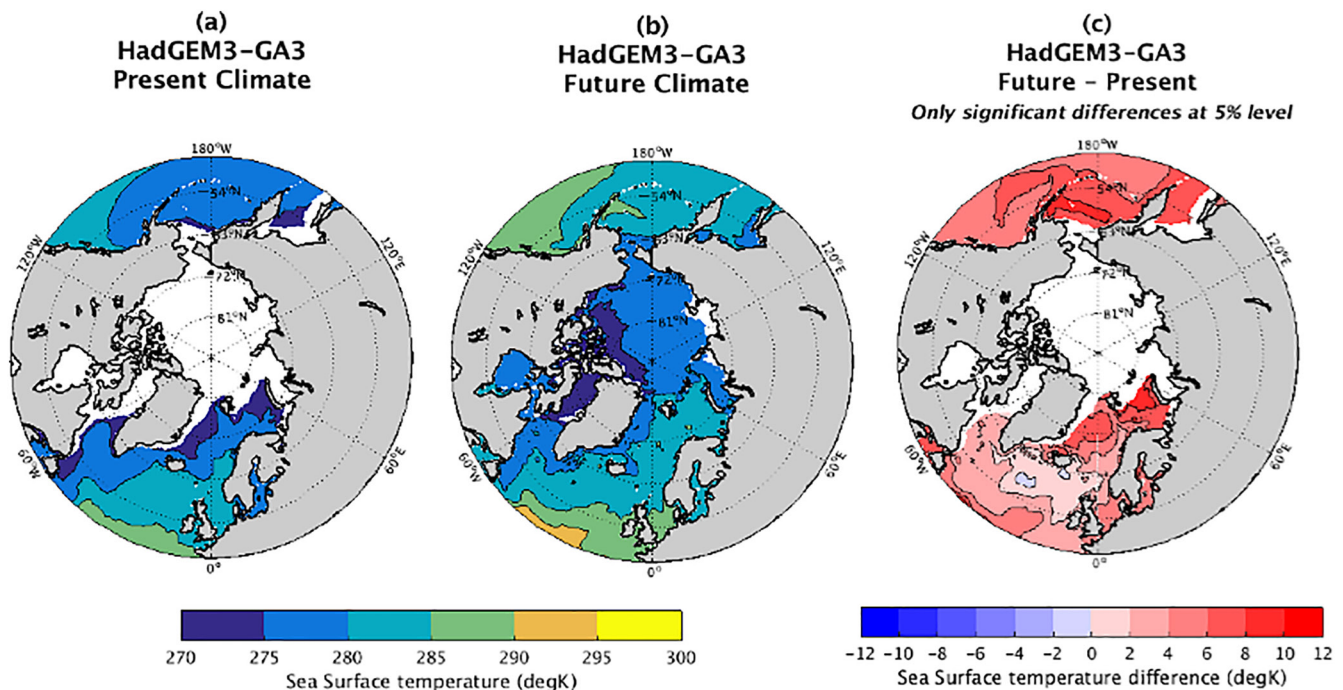


Figure 1. October-March mean sea surface temperature (colored shading) and sea ice covered ocean (sea ice cover > 15%, white areas) in the N512 HadGEM3-GA3 simulations for the present (a) and future (b) climates, and difference between the future and present climates (c). Present day sea ice cover is also reported in panel (c).

the three ensemble members for both historical (1985–2010) and future (2085–2110) climate conditions at 25 km (N512) horizontal resolution, with 85 vertical levels, are analyzed during the cold-season (October–March). The historical climate simulations (1985–2010) are forced with daily SSTs and sea ice from the Operational Sea Surface Temperature and Sea Ice Analysis (OSTIA) product (Donlon et al., 2012). The future SSTs and Sea Ice Fraction (SIF) are derived from the climate change simulations of the HadGEM2-ES Earth System Model for the Representative Concentration Pathway 8.5 (RCP8.5) emissions scenario used for the Intergovernmental Panel on Climate Change Fifth Assessment Report (IPCC AR5, Riahi et al. (2011)). In particular, the future SSTs are calculated by adding the SST changes between 1990–2010 and 2090–2110 from HadGEM2-ES (Collins et al., 2011) to the OSTIA SSTs from the present day climate (i.e., $SST_{future} = SST_{present} + \Delta SST_{future-present}$). The future sea ice concentrations are taken directly from the HadGEM2-ES simulations under the RCP8.5 scenario (Mizielinski et al., 2014). For the regions that entirely lose their sea ice cover between the present and future climates, the SSTs were directly interpolated from the HadGEM2-ES future climate simulations.

Figure 1 shows the SSTs and sea ice used to force the HadGEM3-GA3 simulations for the present and future climate conditions, together with the difference future minus present (significant difference at 5% level, under a standard one-sample *t*-test). The SSTs in the future RCP8.5 scenario (Figures 1b and 1c) are generally warmer by a few Kelvin degrees over most of the North Atlantic (NA). In the Norwegian and Barents Seas, the SSTs are warmer by 2–8 K. In the future RCP8.5 scenario, the winter Arctic SIF is also reduced substantially, to almost completely disappeared. The large decrease in SIF is consistent with, but at the upper-end of, the range of sea ice projections in the CMIP5 models for this scenario (Huang et al., 2017).

These simulations benefit from a horizontal resolution (25 km) which is at the upper end of the recent High Resolution Model Intercomparison Project (HighResMIP), part of the sixth phase of the Coupled Model Intercomparison Project (CMIP6; Eyring et al., 2016; Haarsma et al., 2016). However, a key difference is that the HadGEM3-GA3 data set consists in atmosphere-only simulations, whereas the HiResMIP and the CMIP6 have fully coupled simulations. The lack of coupling could lead to some limitations in the representation of PLs and the large-scale environment. Nonetheless, this study demonstrates that the HadGEM3-GA3 present-day simulations show a similar PLs activity with both the literature and with a coupled reanalysis data set. In particular, in order to assess the representation of PLs in the HadGEM3-GA3 model, PL activity in the present-day climate simulations are compared with those identified in the National Centers for Environmental Prediction

Climate Forecast Systems (NCEP-CFS, Saha et al. (2010)) reanalysis (1979–2010) and the NCEP-CFSv2 Operational Analysis (2011–2014). The two NCEP datasets are based on the same assimilation system and concatenated to span the same time period covered by the climate model simulations. The NCEP-CFS has a horizontal resolution of 38 km (64 vertical vertical levels) and has been chosen for its high spatial resolution, which is relatively close to that of HadGEM3-GA3. The even higher-resolution ERA5 reanalysis (horizontal resolution of 31 km) was not available at the time this analysis began, but future studies will benefit from using it. However, the NCEP-CFS is the only available coupled reanalysis, and its long time period allows a long term comparison of PLs between NCEP-CFS and HadGEM3-GA3.

2.2. Polar Lows Tracking and Identification Scheme

In order to track and identify PLs, this study makes use of the methodology presented and validated in Zappa et al. (2014). Using an objective tracking and identification scheme based on criteria applied to the 850 hPa vorticity, the 10-m wind speed and a measure for the static stability, Zappa et al. (2014) showed that 55% of the 2008–2011 PLs from the observational STARS data set (Noer et al., 2011) could be automatically detected in European Centre for Medium-Range Weather Forecasts (ECMWF) ERA-Interim (Dee et al., 2011) reanalysis data (~80 km resolution) and up to 70% of the STARS events were detected in the ECMWF operational analysis (~9 km resolution). This highlights how PLs are detectable in datasets of sufficiently high spatial resolution. This tracking and identification scheme for PLs has also been used in other studies, such as Yanase et al. (2016), Smirnova and Golubkin (2017) and Stoll et al. (2018), showing valuable skill in identifying and tracking PLs in other regions and reanalysis datasets. A summary of the tracking scheme and identification criteria can be found below and more information can be obtained from Zappa et al. (2014).

The objective feature-tracking algorithm TRACK (Hodges, 1994, 1995, 1999) is used to track PLs from both the model and the reanalysis data, via the 6-hourly relative vorticity at 850 hPa. Prior to applying the tracking, the data is spectrally filtered to retain the spherical harmonic of wave numbers T41–100, which enables the identification to focus on the spatial scales typical of PLs (~400–1,000 km) and to provide some smoothing to reduce the high frequency noise present in the vorticity field. The cyclones are first identified as maxima in the filtered vorticity field that exceed $2 \times 10^{-5} \text{ s}^{-1}$ (Zappa et al., 2014) and initialized into tracks using the nearest neighbor technique. The tracks are then refined using a constrained minimization of a cost function for track smoothness (Hodges, 1995, 1999). Following the tracking, additional fields are added to the tracks in order to apply the following identification criteria for PLs (Zappa et al., 2014):

1. The T41-T100 vorticity at 850 hPa has to be greater than $6 \times 10^{-5} \text{ s}^{-1}$
2. The 10-m wind speed maximum, within a 2.5° radius around the vorticity maxima, has to be greater than 15 ms^{-1} , and has to occur within the search area (and not on the border)
3. The difference in $\Delta T = T_{500} - \text{SST}$, averaged over a 1° radius, has to be less than -43 K
4. The ocean fraction, averaged over a 1° radius, has to be greater than 75%

This set of criteria aids the identification of PLs by searching for their distinguishing characteristics: PLs are intense cyclones associated with gale force winds with a small radius (criteria a and b, Rasmussen and Turner (2003); pages 11–12; Kolstad (2006); Zappa et al. (2014); Yanase et al. (2016); Smirnova et al. (2016); Smirnova and Golubkin (2017); Stoll et al. (2018)), they tend to form in a convectively unstable atmosphere (criterion c, Rasmussen and Turner (2003); page 12; Noer et al. (2011)), and predominantly form over the ocean (criterion d, Rasmussen and Turner (2003); page 13). While the adopted thresholds are partly empirical, they have shown good skill in isolating PLs in different regions and datasets. However, while the value of -43 K on the vertical temperature difference has been successfully used in previous PL studies (Zahn & von Storch, 2008; Xia et al., 2012; Yanase et al., 2016), it has also been shown to lead to the exclusion of some PLs forming under forward shear conditions in the North Atlantic (Stoll et al., 2018; Terpstra et al., 2016). Recent studies have introduced new PLs identification schemes, including a criterion on a new CAO index and information on PLs vertical wind shear vector (Meyer et al., 2021; Stoll et al., 2021; Terpstra et al., 2021), that can improve the detection of PLs, particularly for forward shear conditions. On the other hand, Radovan et al. (2019) investigated PLs development from the observational data set of PLs over the Nordic Seas from Noer and Lien (2010), and found that not one condition was the most relevant for PL formation or growth. Although those new identification criteria are

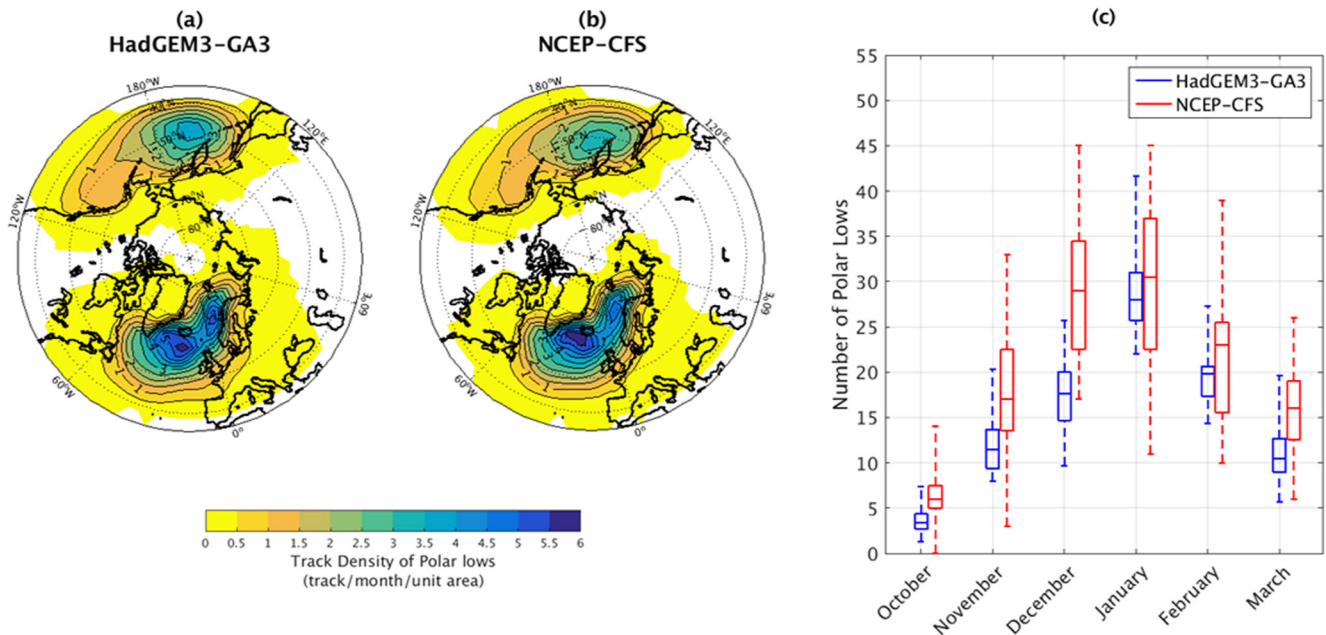


Figure 2. NH October-March track density of PLs based on HadGEM3-GA3 N512 present-day climate model (a) and NCEP-CFS reanalysis (b), and seasonal cycle of PL numbers (c) in HadGEM3-GA3 N512 climate model (blue) and NCEP-CFS reanalysis (red). Track densities are calculated in number per month per 5° spherical cap (10^6 km^2). The boxplots represent the median, 25th and 75th percentiles and the extreme data points.

not tested in this study, we will show that the PLs climatology obtained by our approach is broadly comparable to those obtained from these more recent approaches.

The tracking is carried out for October to March since this is when nearly all PLs occur in the NH (Rasmussen and Turner (2003), pages 79-96-98), for a 26-year period (1985–2010) for the three ensemble members of the HadGEM3-GA3 climate model and for a 36-year period (1979–2014) for the NCEP-CFS.

3. Present-Day Representation of Polar Lows

In this section, the representation of NH PLs identified in the high-resolution simulations of the HadGEM3-GA3 climate model and in the NCEP-CFS reanalysis is assessed and compared to the available literature based on both observational- and model-based studies. Since there is no real truthful global PLs data set and since there is still a large disagreement between different observational and reanalysis datasets regarding PL characteristics (such as the vertical temperature difference or the maximum wind speed), our results will also be compared against those obtained from another global reanalysis-based climatology of PLs based on different identification criteria and datasets (Stoll et al., 2018).

The mean and inter-annual standard deviation of PL numbers identified over the NH in the NCEP-CFS reanalysis are 120.8 and 18.3 PL per year. The October to March track density for the NH PLs from the reanalysis (Figure 2b) shows three maxima in the PL track density: one south of Iceland, one over the Norwegian Sea and one east of the Sea of Okhotsk. These regions are some of the most favorable for PLs formation since they are often collocated with strong temperature and wind gradients (Rasmussen and Turner (2003), pages 64–66). A similar spatial distribution of PLs were also found in Stoll et al. (2018) (with both the ASR and ERA-I reanalyses), with the main difference being a slightly stronger maximum in the gulf of Alaska in Stoll et al. (2018). The PLs seasonal cycle was also assessed (Figure 2c) and shows that NH PL numbers increase from October to December-January and then progressively decrease through to March. In particular, monthly mean PL numbers using NCEP-CFS reanalysis range from around 6 PLs in October to a maximum of 30 PLs in January. With the ERA-I and ASR reanalyses, Stoll et al. (2018) found a seasonal distribution of NH PLs peaking in December and January. This shows that our climatology based on NCEP-CFS is comparable to that obtained in Stoll et al. (2018) with the ERA-I and ASR reanalyses, despite the use of different identification criteria. While observational satellite-based

studies are also available, they are only regionally focused and often cover too short time periods to characterize the global seasonal cycle of PLs. Nonetheless, for the Nordic seas, with the only exception of Rojo et al. (2015), they also tend to suggest a seasonal maximum between December and January (Blechschmidt, 2008; Bracegirdle & Gray, 2008; Noer et al., 2011). Overall, these results suggest that our climatology captures a spatial distribution and seasonal cycle of PLs which are comparable with that presented in previous studies.

The cold-season mean and inter-annual standard deviation of PL numbers from the three ensemble members of the HadGEM3-GA3 climate model are 93.4 and 8.1 PL per year respectively. The mean numbers from HadGEM3-GA3 and NCEP-CFS are significantly different at the 5% level (difference of means performed with two-sample *t*-test), suggesting that the HadGEM3-GA3 model underestimates the number of PLs identified in the NCEP-CFS reanalysis by about 20%. Nonetheless, Figure 2 shows that both the October to March track density of NH PLs and the seasonal cycle of PL numbers for the present-day climate from HadGEM3-GA3 reproduce well that obtained in the NCEP-CFS reanalysis. In particular, the spatial distribution of track density in the HadGEM3-GA3 model is very similar to that found in the NCEP-CFS reanalysis, although the maxima are lower than observed. Likewise, the seasonal cycle of PL numbers in HadGEM3-GA3 shows an increase from October to January and then a decrease until March, with monthly PL numbers in HadGEM3-GA3 ranging from around 3 PLs in October to 28 PLs in January. These results are comparable to those found using the NCEP-CFS reanalysis, and indicate similarities in the seasonal cycle and spatial distribution of PLs in the two datasets.

To further investigate the representation of PLs in the HadGEM3-GA3 model, other characteristics of PLs have been assessed and compared to NCEP-CFS. These characteristics are the along-track vorticity, the 10-m wind speed and the vertical difference in temperature ($\Delta T = T_{500} - SST$) found at the maximum vorticity of each PL. Both the HadGEM3-GA3 model and the NCEP-CFS reanalysis show very similar statistics regarding PL characteristics. The mean of the PLs maximum vorticity is found to be $8.5 \times 10^{-5} \text{ s}^{-1}$ for HadGEM3-GA3 (resp. $8.3 \times 10^{-5} \text{ s}^{-1}$ for NCEP-CFS). The mean of the maximum wind speed is 20.5 ms^{-1} for HadGEM3-GA3 (resp. 20.5 ms^{-1} for NCEP-CFS), and the mean temperature difference is -45.5 K for HadGEM3-GA3 (resp. -45.1 K for NCEP-CFS). These results confirm the fidelity of the representation of present-day PL characteristics in the HadGEM3-GA3 model. Although Chen and von Storch (2013) found a small positive trend in PL numbers (less than 1 PL/year for the 1948–2010 period), this study, along with other long-term PL studies such as Zahn and von Storch (2008) (period: 1948–2006), Michel et al. (2018) (period: 1979–2014) and Stoll et al. (2018) (period: 1979–2016), found no significant trends in PL numbers in either HadGEM3-GA3 present-day simulations or in the NCEP-CFS reanalysis. Finally, PLs duration has been analyzed and showed that HadGEM3-GA3 PLs have a typical lifetime of 25 hr (standard deviation: 14 hr), with 50% of the PLs lasting less than 24 hr and 91% of PLs lasting less than 48 hr. The NCEP-CFS PLs have a mean lifetime of PLs of 30 hr (standard deviation: 18 hr). These results are relatively similar to the literature using observational and reanalysis datasets, which span from a mean lifetime of around 15 hr (Laffineur et al., 2014; Smirnova et al., 2016) with more than 70% of PLs lasting less than 30 hr (Rojo et al., 2015).

In summary, the results presented here suggest that, (a) the detection of PLs in NCEP-CFS is found to be within the uncertainty range of previous studies using observational data and reanalyses, and (b) the representation of present-day PLs in the HadGEM3-GA3 model is found to be reasonably close to those in the NCEP-CFS reanalysis. Hence these results suggest it is reasonable to use the projections from the HadGEM3-GA3 model to understand how PLs number and spatial distribution may change with climate change.

4. How Are Polar Lows Projected to Change in the Future in HadGEM3-GA3?

This section will first investigate the response of PLs to climate change, in their number, characteristics and spatial distribution. This section will also explore the synoptic conditions around PLs by analyzing the differences in large-scale fields between the present and the future climate conditions.

4.1. Polar Lows Response to Climate Change

Between the present-day and the end of the 21st century, the total number of PLs in the NH in HadGEM3-GA3 is found to substantially decrease from 93 PLs per winter season (inter-annual std: 8.1) in the present-day climate to 35 PLs per winter season (inter-annual std: 5.1) in the future climate under the RCP8.5 scenario. This represents a decrease of more than 62% in PL activity. The sensitivity of the response in PL numbers to the

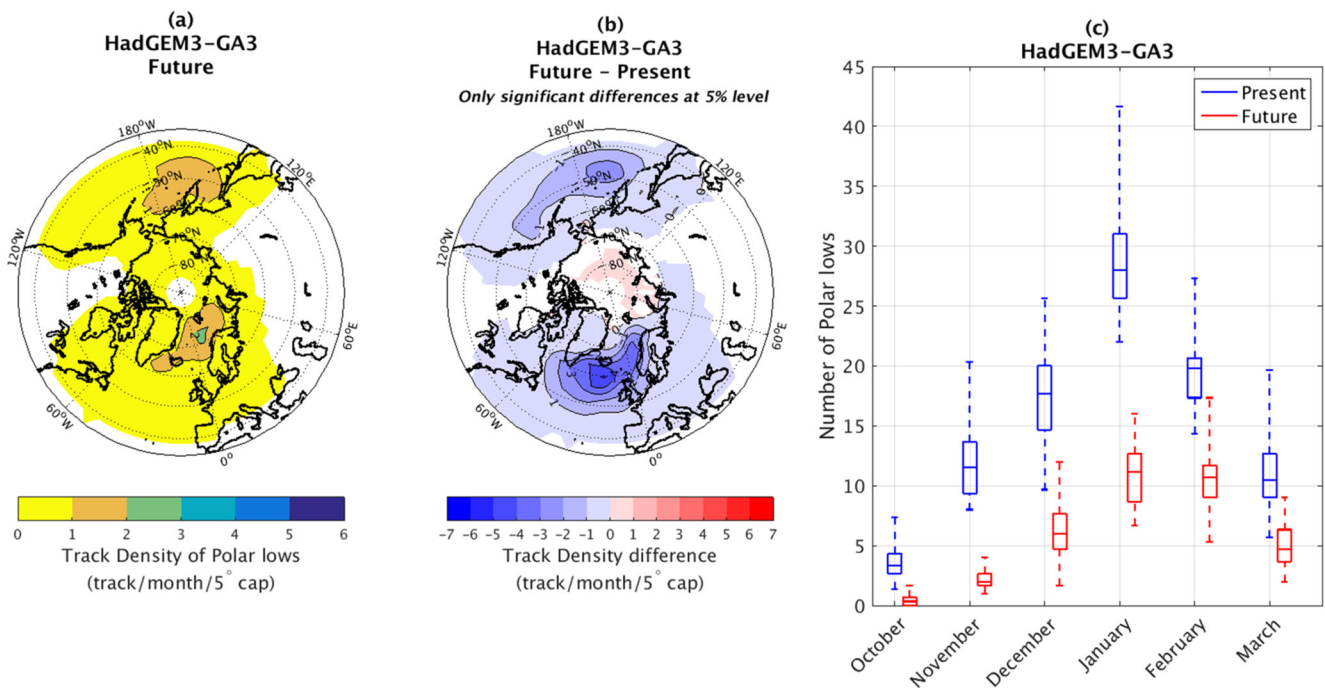


Figure 3. NH October-March track density of the ensemble mean of PLs in the HadGEM3-GA3 climate model for the future climate (a) and difference (significant at 5% level) between future and present climates (b), and ensemble mean seasonal cycle of PL numbers (c) averaged over the three 26-year ensemble members of the HadGEM3-GA3 climate model for the present (blue) and future (red) climates. Track densities are in track per month per 5° spherical cap (10^6 km^2). The boxplots represent the median, 25th and 75th percentiles and the extreme data points.

identification criteria under climate change is further investigated in Section 4.1.1. The changes in PL characteristics between the present and future climates have also been assessed. The mean of the maximum 850 hPa vorticity distribution is found to decrease from 8.5 to $7.9 \times 10^{-5} \text{ s}^{-1}$. Similarly, the mean of the wind speed intensity distribution is also found to decrease from 20.5 to 18.9 ms^{-1} , which suggests that particularly intense PLs may also become less frequent in the future. Additional information on changes in PL characteristics is presented in the Supporting Information S1. Furthermore, a small increase of 2.6% of the mean duration of PLs is found in the future climate. This increase, is found to be mainly due to long-lasting PLs (i.e., lifetime $>72 \text{ hr}$) and thus does not seem to affect PLs with regular 1-to-2-day lifetime.

Figure 3 shows spatial maps of the ensemble mean track density of PLs in the HadGEM3-GA3 simulations for the future climate, and the difference between the future and the present climates. For the significance testing for the difference of track densities of PLs, the permutation approach to significance (Hodges, 2008) is used. Regions of present-day PL activity in the climate model simulations (i.e., the high-latitude NA, the Nordic Seas and the region around the Sea of Okhotsk) continue to be regions of PL activity in the future. However, Figure 3b indicates that PL activity in all three regions is much reduced under climate change. Over the central Arctic Ocean as well as over the seas along the Russian coastlines (i.e., Kara, Laptev and East Siberian Seas), a significant increase in PL activity is seen although it is a small change in absolute magnitude (+1 PL per month per 5° spherical cap). Figure 3c shows that a shift in the seasonality in PL activity toward late winter is seen in the climate change simulations, with a shift of the peak in PL activity from predominantly January to both January and February (i.e., January and February mean PL numbers of 29.1 and 19.8 respectively for the present-day scenario, and 11.0 and 10.4 PLs in January and February respectively for the future scenario). This shift in PLs seasonality could be due to the future Arctic sea ice maximum extent also shifting toward the end of winter (Landgren et al., 2019). A future decline of Arctic sea ice extent could hence prevent future CAO event, leading to a decrease of PLs future activity (Mallet et al., 2017).

As described in the introduction, the projected decrease of PL numbers over the NA Ocean at the end of the 21st century has also been reported in previous studies with projected changes ranging from -5% to -53% (Zahn & von Storch, 2010; Chen et al., 2014; Romero & Emanuel, 2017; Landgren et al., 2019). Although previous studies

Table 1

Sensitivity of the Mean Number and Inter-Annual Standard Deviation of PLs Found in the NH With the N512 HadGEM3-GA3 Model for Both Present and Future Climate Conditions, to Adopting Different Identification Criteria

	Present climate		Future climate		Percentage of change
	Mean nb.	Std. dev.	Mean nb.	Std. dev.	
Control	93.4	8.1	35.2	5.1	−62.1%
$\xi > 0 \times 10^{-5} \text{ s}^{-1}$	156.7	14.6	47.3	5.0	−69.8%
$\xi > 9 \times 10^{-5} \text{ s}^{-1}$	30.6	5.1	3.6	1.3	−88.1%
$WS > 0 \text{ ms}^{-1}$	102.4	10.4	30.2	4.0	−70.5%
$WS > 18 \text{ ms}^{-1}$	69.3	8.9	10.0	2.0	−85.6%
$\Delta T < -39 \text{ K}$	210.0	15.0	60.4	5.6	−71.2%
$\Delta T < 0 \text{ K}$	674.1	23.0	353.9	16.9	−47.5%

Note. Control refers the standard setup, while in the other rows either the vorticity (“ ξ ”, with values higher than 0 or $9 \times 10^{-5} \text{ s}^{-1}$), the wind speed (“WS”, with values higher than 0 or 18 ms^{-1}) or the temperature difference (“ $\Delta T = T500 - SST$ ”, with values lower than -39 or 0 K) criteria are perturbed one at a time.

show different responses in the analyzed models, focus on different regions and use different PLs identification methods as well as emissions scenarios, all are in accordance regarding a future decrease of PLs numbers with additional changes in spatial distribution and seasonal cycle. Thus a robust reduction in PL activity due to climate change is seen across several climate model studies. Therefore, the decrease in PLs in the high-resolution HadGEM3-GA3 simulations confirms, while being at the upper end of the projected change, these previous studies. Understanding the cause of the large uncertainty in the magnitude of the change, such as the role played by the use of different identification methods, study regions, climate models and emissions scenarios, is an outstanding question for future research (see Summary and Conclusion section).

The regional climate model domain used in Landgren et al. (2019) also included the Barents Sea, where they noted a small but significant increase in PL activity in their climate change simulations, due to the sea ice retreat in this region. The significant increase in PL activity along the sea ice edges in the Barents Sea in response to climate change is also seen in the HadGEM3-GA3 model. This future increase in the Barents Sea could be of substantial impact for future planned oil and gas activities (Greaker & Rosendahl, 2017), and for tourism activities, such as cruise ships (Palma et al., 2019), in the region. However, since the HadGEM3-GA3 simulations are global in nature, we also note that there are significant increases in PL activity over most of the Arctic,

including the Kara Sea and the Bering Strait. In addition, increased PL activity ($+0.5$ – 1 PL per month) in the climate model simulations was also seen in other regions, such as the Hudson Bay, and the Beaufort Sea, although these are not statistically significant at the 5% significance level (however they are significant at the 10% level). These results indicate that new regions of PL activity may appear under climate change. In Section 4.2, the relationship between changes in PL activity and the large-scale environment are explored.

4.1.1. Sensitivity of the Future Response in PL Numbers to the Identification Criteria

For the changing climate, one question that arises is whether the response in the number of PLs is sensitive to the exact thresholds used for the identification of PLs. To answer this question we examine how sensitive the response in the number and characteristics of PLs is to perturbations in the identification criteria used in this study. Table 1 summarizes the results for the mean numbers and the inter-annual standard deviations of NH PLs found for the present and future climate conditions. In particular, the first row “Control” represents the setup used in this study for PL identification (i.e., a maximum vorticity greater than $6 \times 10^{-5} \text{ s}^{-1}$, a maximum wind speed greater than 15 ms^{-1} and a minimum temperature difference ΔT lower than -43 K). The other rows show the results when each criterion, one at a time, is either relaxed or made more stringent.

As previously mentioned, a future decrease of 62% of PL numbers is found over the NH in the HadGEM3-GA3 simulations. Variations in the future decrease in PL number (−47% to −88%) is found depending on the adopted identification criteria. However, the results from Table 1 suggest that a broadly large decrease in PL number is found in the climate model simulations. Previous results (Landgren et al., 2019) also showed that future PL numbers were still expected to decrease even with lowered identification criteria thresholds (especially the static stability criterion). This implies that our conclusion of a future reduction in PLs number is robust to the exact choice of identification criteria. Furthermore, the percentage drop is larger when adopting more stringent criteria on wind speed and vorticity intensity. Such a tendency toward an overall weakening of the PLs is confirmed by exploring the dependence of PL characteristics on the identification criteria in both present and future simulations (see Supporting Information S1). The PL mean vorticity, wind speed and absolute vertical temperature difference values are found to decrease under climate change, irrespective of the threshold values chosen for the PLs identification criteria. If the dynamics of PLs were to change in a warmer climate, for example, thanks to the larger atmospheric moisture content, it cannot be excluded that PLs would start to form in different environmental conditions, so that the -43 K threshold here used for identification becomes too much (or too little) stringent. The strong weakening of PLs identified here, and the consistence with previous studies, suggests that a future reduction in PLs activity is likely to be robust, but to further increase the confidence, future research

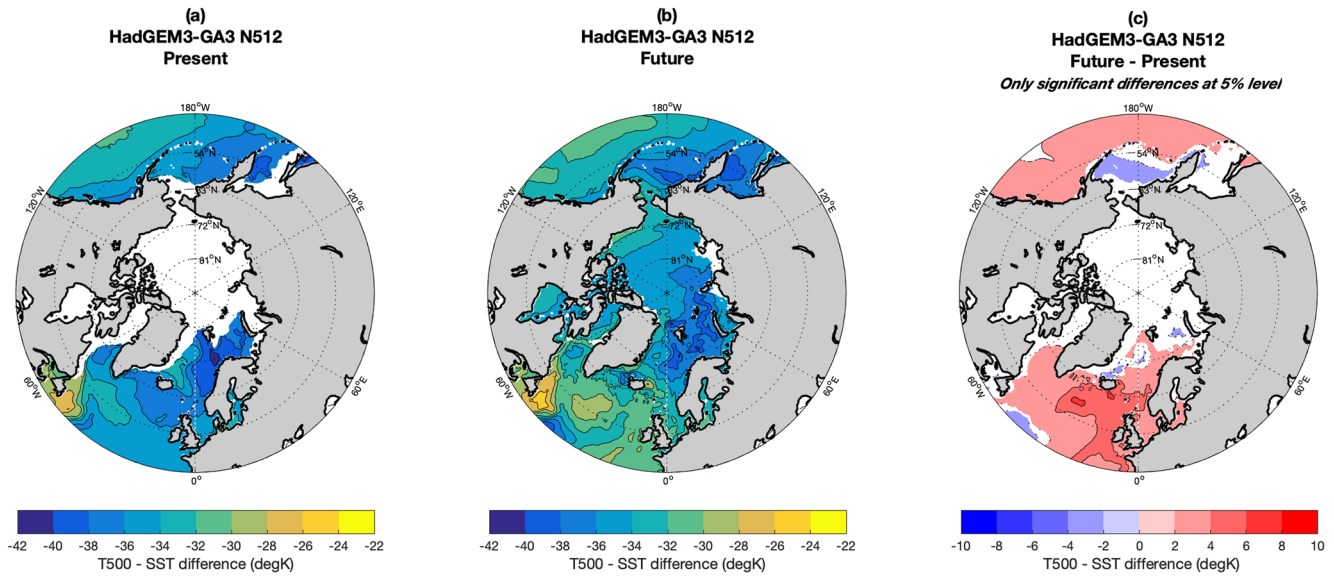


Figure 4. October-March ensemble mean atmospheric temperature difference ($\Delta T = T500 - SST$, in K) from the HadGEM3-GA3 climate model for the present (a) and future (b) climates and for the difference (significant at 5% level) between the future and present climates (c). The white areas of the maps represent the locations of the present and future climate Arctic sea ice.

should consider quantifying the climate change response using the more recent PLs identification criteria (Meyer et al., 2021; Stoll et al., 2021).

4.2. Large-Scale Environment

Arctic sea ice is projected to decrease under climate change (J. Stroeve et al., 2007; J. C. Stroeve et al., 2012) and atmospheric static stability is expected to increase (Zahn & von Storch, 2010; Woollings et al., 2012; Mallet et al., 2017). Both of these changes in the large-scale environment may potentially impact on PL activity in the future.

Figure 4 shows the NH atmospheric vertical temperature difference ΔT (i.e., $T500 - SST$) in HadGEM3-GA3 for the present and future climates and the differences between the two. An overall increase of the static stability between the present and future climate in the climate model simulations can be seen in Figure 4c, with an average NH wintertime increase by 2 K. However, there are larger increases over the NA Ocean and the Norwegian Sea. Zahn and von Storch (2010), Woollings et al. (2012) and Mallet et al. (2017) found that the increase in atmospheric static stability is due to the faster increase of the future mid-tropospheric temperatures relative to the SSTs, which is also the case in HadGEM3-GA3 (around +2 K for NA SST and around +6 K for NA T500, not shown). These differences in surface and mid-tropospheric warming arise since the mid-tropospheric temperature increase is strongly correlated with mean global warming, while the increase in surface temperatures are related to changes in the AMOC and the sea ice melt (Gervais et al., 2018; Woollings et al., 2012). This increase in the atmospheric stability leads to less favorable conditions for PLs over the NA Ocean (Mallet et al., 2017). The number of PLs is also seen to decrease (see Figures 3 and 4) in regions which become slightly more unstable and which appear sea-ice free in the future (e.g., Bering Sea, Labrador Sea, eastern coast of Greenland), hence suggesting that other mechanisms may also be playing a role (see below). Similarly to the northern Atlantic Ocean, the Pacific Ocean is seeing a future increase in static stability, however weaker. In some regions, a decrease in future temperature difference static stability (i.e., negative anomaly of temperature difference) can be seen, indicating that the surface warming is higher than the mid-troposphere warming. This occurs close to regions of sea ice loss (i.e., along the sea ice edge over the Nordic Seas and over the Bering and Okhotsk Seas), and it is consistent with the faster warming of high-latitude SSTs linked to the polar amplification of global warming.

Furthermore, the occurrence of extreme temperature difference (ΔT) conditions also increases in the future. Figure 5 shows the 2.5th percentile of the monthly atmospheric temperature difference ($\Delta T = T500 - SST$, in K) from the the climate model simulations for the present and future climate conditions, and the difference

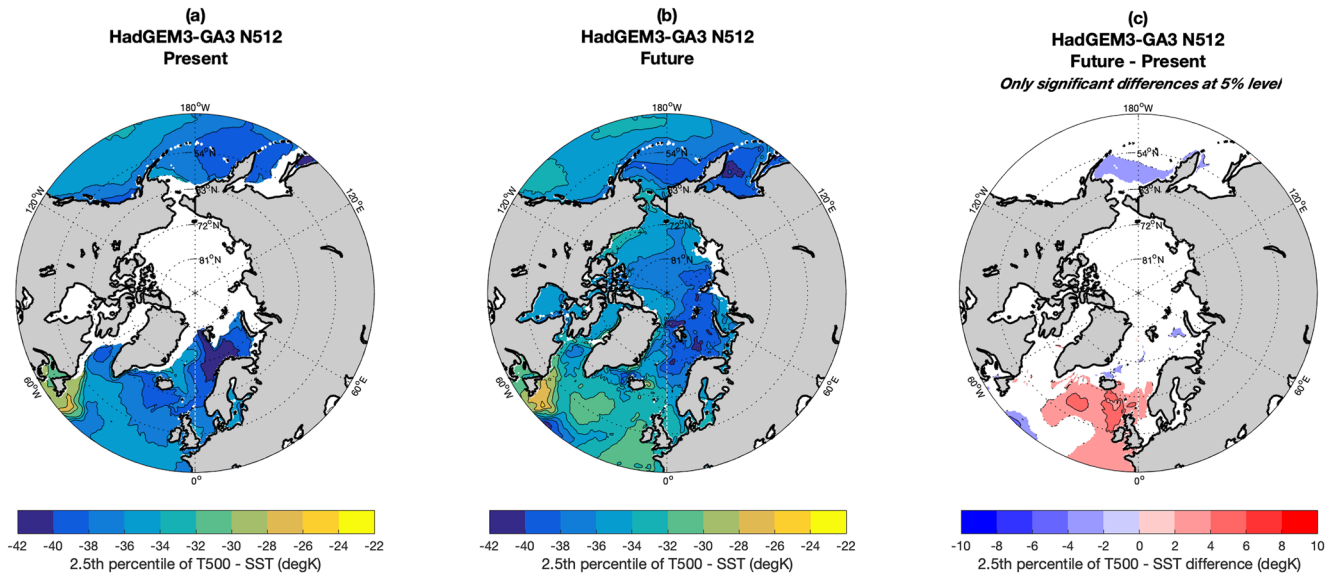


Figure 5. 2.5th percentile of the atmospheric temperature difference ($\Delta T = T500 - SST$, in K) for the present (a) and future (b) climate scenario, and for the difference (significant at 5% level) between the future and the present climate (c) found from October to March in the HadGEM3-GA3 climate model.

(significant at 5% level, under a standard one-sample *t*-test) between the future and present. These results show that the frequency of atmospheric states associated with an extremely unstable atmosphere is expected to happen less often in the future climate, particularly in the NA ocean. The regions showing a reduction of ΔT in the mean, for example, the Bering sea and the sea ice edge along the Nordic sea, do not show significant changes in the frequency of extreme ΔT occurrences. Overall this shows that regions with frequent PLs development will encounter a predominant decrease in the mean and extreme environmental conditions favorable to their development in HadGEM3-GA3.

Another large-scale environmental variable that could explain the future decrease of PLs is the baroclinic instability. A useful local measure for baroclinic instability, and hence for potential PL development, is the maximum Eady growth rate (EGR, Hoskins and Valdes (1990)): $EGR = 0.31 * (f/N) * (dU/dz)$, with *f* is the Coriolis parameter, *N* the Brunt-Väisälä frequency, *U* is the wind speed and *z* is the geopotential height. The mean October-March EGR, shown in Figure 6, here computed for monthly values between 850 and 500 hPa, for the historical and future climate scenarios, and the difference (significant at 5% level, under a standard one-sample *t*-test) between the future and the present climate conditions. The EGR is found to decrease drastically over the Nordic and Labrador Seas, the Bering Strait and the North Pacific Ocean under climate change (Figure 6c). These results suggest that baroclinicity also decreases up to 0.2 days⁻¹ in the regions of current PL development which suggests reduced baroclinicity may also play a role in reducing PL numbers. On the other hand, the EGR is found to slightly increase in the future climate scenario over the North Sea and the most north-eastern part of the NA Ocean, but these are not common regions of PL formation. Although not significant at the 5% level, an increase in the EGR is also found over the Arctic Ocean (not shown), which is also among the regions of possible future increase in PLs shown in Figure 3, indicating that a possible EGR increase over the Arctic could contribute to new location of PLs.

Another variable which could provide insight on the future PLs decline is the vertical atmospheric wind shear, which is used in the EGR calculation. The analysis of this variable shows a very similar pattern of change, including the sign, to that found for the EGR (not shown). This implies that changes in wind shear, rather than static stability, dominate the response in the EGR. In particular, the results show a decrease in future vertical wind shear over the Nordic Seas, which is the current main region for PL activity, and over the East Siberian Sea and the north-east Pacific Ocean. Furthermore, an increase of the vertical wind shear is found over the North Atlantic Ocean. These results confirm that the PLs future decrease might be due to different large-scale environmental factors, including both the vertical and horizontal temperature and wind gradients.

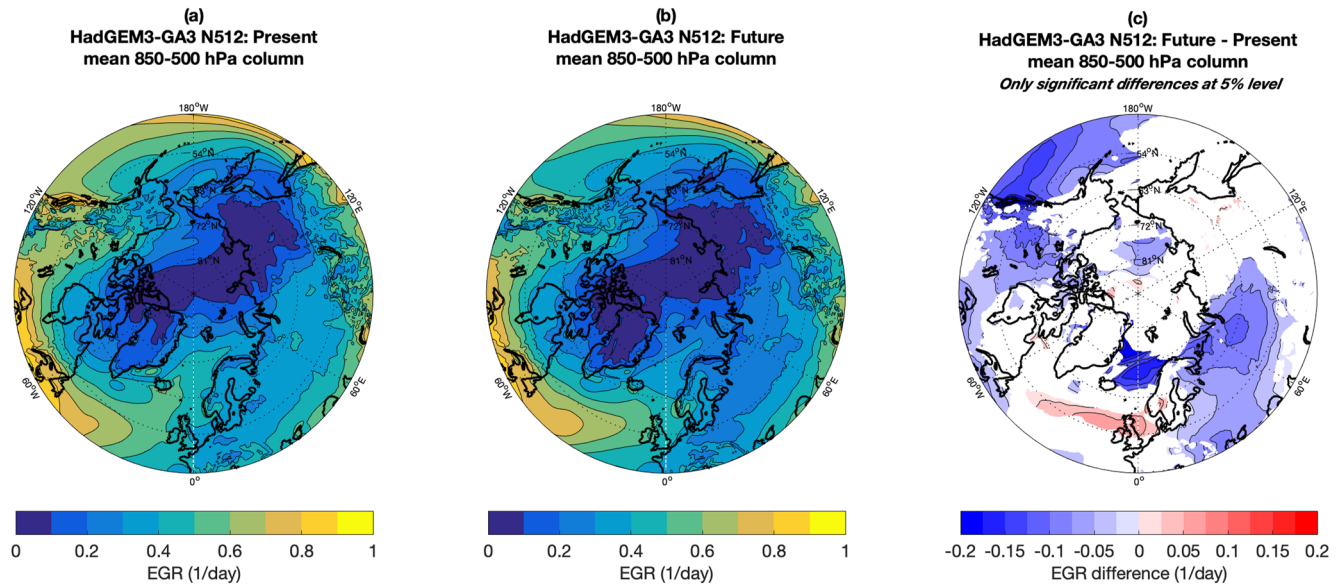


Figure 6. Mean Eady growth rate for the present (left panel) and future (middle panel) climate scenario, and for the difference between the future and the present climate (right panel) found from October to March in the HadGEM3-GA3 climate model.

In summary, an increase of both average and extreme ΔT occurrences is expected in the future, reinforcing the previous findings showing that PLs future decrease is linked to a future increase in atmospheric stability. In particular, the occurrences of PLs will be influenced by both the future increase of the mean and extreme values of ΔT , as well as a decrease of baroclinic instability. Comparing the patterns in the spatial maps of the changes suggests that the increase in static stability tends to dominate the weakening of PL activity in the North Atlantic and Pacific ocean, while the reduction in baroclinicity may be more important in the Norwegian Sea. However, along with the projected decrease of the sea ice (J. Stroeve et al., 2007; J. C. Stroeve et al., 2012), the potential increase in atmospheric static stability (Zahn & von Storch, 2010; Woollings et al., 2012; Mallet et al., 2017) and decrease of baroclinic instability are not the only environmental changes which will occur over the Arctic regions under climate change. Other changes may also affect PLs future activity, such as, in particular, the likely increase of the moisture content over the Arctic due to the fast warming of the region, the changes in surface wind speed/direction, the slowdown of the AMOC, etc. Hence, although this study only investigates the previously mentioned climate components, a number of other factors should also be taken into account for future research on PL activity under climate change.

5. Summary and Conclusion

Polar Lows (PLs) are one of the key weather risks that impact on infrastructure, shipping and coastal communities in the Arctic. In this study, the response of PLs to climate change has been assessed for the first time in a high-resolution (25 km) atmosphere-only global climate model (N512 HadGEM3-GA3, Mizieliński et al. (2014)). Using a high-resolution global climate model allows to investigate PL characteristics over the whole NH and to assess their interaction with the large-scale environment, while decreasing the possible bias that may occur due to the use of regional climate models. PLs are identified using an objective tracking and identification scheme (Zappa et al., 2014) and their representation in HadGEM3-GA3 is evaluated using the NCEP-CFS reanalysis. The main findings of this study are:

1. The seasonal cycle and spatial distribution of PLs in the HadGEM3-GA3 model are found to be very similar to those in the NCEP-CFS reanalysis, although the model underestimates the total number of PLs compared in the NH by approximately 20%. Overall, the representation of PLs seasonal cycle and spatial distribution in HadGEM3-GA3 is also consistent with observational estimates, especially given the large uncertainty in PL numbers found in reanalysis and observational studies (Bromwich et al., 2018; Stoll et al., 2018).

2. The number of wintertime NH PLs is projected to decrease substantially by the end of the 21st century in the HadGEM3-GA3 climate model forced by the oceanic conditions projected in the RCP8.5 scenario by the HadGEM2-ES model. An average decrease of over 60% in total PLs numbers is found with most of the reduction occurring in the North Atlantic (NA), the Nordic Seas and the Sea of Okhotsk. The decrease in PLs number is here attributed to the increase in atmospheric stability and the decrease of the baroclinic growth rate found in these regions. In addition, a shift in the peak seasonal cycle of PL activity from a maximum in January to a January-February “plateau” is found in the HadGEM3-GA3 future scenario, which is consistent with the projected Arctic sea ice loss being less extensive toward the end of winter (Landgren et al., 2019). Furthermore, the most intense PLs are projected to become less frequent, and wind speeds are projected to become less intense.
3. Despite the projected reduction in the overall number of PLs in the NH, new regions of PL activity are found in the future scenario of HadGEM3-GA3 over the Arctic, particularly along the northern Russian coastline (i.e., the Kara, Laptev and East Siberian Seas). The increase in PL activity found over the Arctic Ocean is consistent with the decrease in Arctic sea ice extent (leading to a larger open-ocean area where PLs can form) and the possible increase of the baroclinic growth rate found in this region. These spatial differences found in the future PL activity in the Arctic could hence have considerable impacts on future human activities in the Arctic, including shipping and tourism.

This study confirms previous findings that PL numbers over the NA and the Nordic Seas are projected to decline under climate change, associated with an increase in atmospheric stability. The results over the NA and the Nordic Seas are comparable to (but larger than) those found in previous studies using regional climate models and statistical-dynamical methods. Previous studies have reported possible future decreases in PL numbers over the NA and the Nordic Seas of approximately 10%–50% (Zahn & von Storch, 2010; Romero & Emanuel, 2017; Landgren et al., 2019). The larger PLs response found in the HadGEM3-GA3 simulations may be the result of the large Arctic sea ice response to climate change seen in HadGEM2-ES, which provides the boundary conditions for the atmospheric-only HadGEM3-GA3 global climate model simulations. In addition, the global nature of the HadGEM3-GA3 simulations in this study has enabled us to investigate in a physically consistent way the projected response of PLs to climate change in different regions of the NH. In particular, the increase in wintertime PL activity over the Arctic basin has only been reported once before (Landgren et al., 2019).

A key direction for future research is to further understand the reasons for the large uncertainty in the projected responses of PLs to climate change. Given that previous studies have been carried out with different modeling methods and scenarios, one way forward would be to investigate the projected responses in an ensemble of climate models forced with comparable conditions and scenarios. In this regard, the inter-comparison of PLs in the HighResMIP experiments (a set of simulations using high-resolution global coupled climate models at approximately 25–50 km resolution) may prove to be insightful. Furthermore, although this study makes use of a state-of-the-art global climate model, some limitations, both in the representation of PLs (trajectory, wind speed, vertical temperature gradient, etc.) and the large-scale environment (SST and surface energy fluxes feedback, thermodynamical properties of the atmosphere, etc.), could arise from using an atmospheric-only global climate model. Future research would hence benefit from using fully coupled climate models, such as the ones from the Coupled Model Intercomparison Project Phase 6 (CMIP6) project. Finally, it would be important to improve PL climatologies, with both observational and *in-situ* datasets as well as high-resolution reanalyses (such as the ERA5 and Copernicus Arctic Regional Reanalysis). This would not only help us improve our current understanding of PL characteristics and lifecycle in the present-day climate, but also enhance the accuracy of future projections of PLs under climate change.

Data Availability Statement

The study is based on the UPSCALE data set licensed from the University of Reading, hosted on the JASMIN platform and available at <http://proj.badc.rl.ac.uk/upscale> (met-upscale@lists.reading.ac.uk). The UPSCALE data was produced by a MetOffice-NCAS-CMS collaboration using the HadGEM3 model with support from NERC and the MetOffice and the PRACE Research Infrastructure resource HERMIT. The NCEP-CFS Reanalysis and NCEP-CFSv2 Operational Analysis, developed by NOAA NCEP and from the NOAA Operational Model Archive and Distribution System (NOMADS), are available at <https://www.ncdc.noaa.gov/data-access/model->

data/model-datasets/climate-forecast-system-version2-cfsv2. The feature-tracking algorithm is available at <https://gitlab.act.reading.ac.uk/track/track> (K. Hodges, k.i.hodges@reading.ac.uk). The UPSCALE polar low tracks can be found at <https://researchdata.reading.ac.uk/id/eprint/299> (DOI: <https://doi.org/10.17864/1947.000299>).

Acknowledgments

The work described in this paper has received funding from the European Union's Horizon 2020 Research and Innovation programme through Grant agreement no. 727862 APPLICATE. LS, KH and RS were supported by funding from the National Centre for Atmospheric Science. Finally, we thank the anonymous reviewers for their constructive comments that helped to improve this manuscript.

References

- Blechschmidt, A. M. (2008). A 2-year climatology of polar low events over the Nordic Seas from satellite remote sensing. *Geophysical Research Letters*, 35(9), 2003–2007. <https://agupubs.onlinelibrary.wiley.com/doi/full/10.1029/2008GL033706>
- Bracegirdle, T. J. & Gray, S. L. (2008). An objective climatology of the dynamical forcing of polar lows in the nordic seas. *International Journal of Climatology: A Journal of the Royal Meteorological Society*, 28(14), 1903–1919. <https://rmets.onlinelibrary.wiley.com/doi/abs/10.1002/joc.1686>
- Bromwich, D. H., Wilson, A. B., Bai, L., Liu, Z., Barlage, M., Shih, C.-F., et al. (2018). The arctic system reanalysis, version 2. *Bulletin of the American Meteorological Society*, 99(4), 805–828. <https://doi.org/10.1175/BAMS-D-16-0215.1>
- Chen, F., & von Storch, H. (2013). Trends and variability of north pacific polar lows. *Advances in Meteorology*.
- Chen, F., von Storch, H., Zeng, L., & Du, Y. (2014). Polar low genesis over the north pacific under different global warming scenarios. *Climate Dynamics*, 43(12), 3449–3456. <https://doi.org/10.1007/s00382-014-2117-5>
- Claud, C., Heinemann, G., Raustein, E., & Mcmurdie, L. (2004). Polar low *le cygne*: Satellite observations and numerical simulations. *Quarterly Journal of the Royal Meteorological Society*, 130(598), 1075–1102. <https://doi.org/10.1256/qj.03.72>
- Collins, W. J., Bellouin, N., Doutriaux-Boucher, M., Gedney, N., Halloran, P., Hinton, T., et al. (2011). Development and evaluation of an earth-system model – Hadgem2. *Geoscientific Model Development*, 4(4), 1051–1075. <https://doi.org/10.5194/gmd-4-1051-2011>
- Curio, J., Chen, Y., Schiemann, R., Turner, A. G., Wong, K. C., Hodges, K., & Li, Y. (2018). Comparison of a manual and an automated tracking method for Tibetan plateau vortices. *Advances in Atmospheric Sciences*, 35(8), 965–980.
- Curio, J., Schiemann, R., Hodges, K. I., & Turner, A. G. (2019). Climatology of Tibetan plateau vortices in reanalysis data and a high-resolution global climate model. *Journal of Climate*, 32(6), 1933–1950. <https://doi.org/10.1175/jcli-d-18-0021.1>
- Dee, D. P., Uppala, S. M., Simmons, A. J., Berrisford, P., Poli, P., Kobayashi, S., et al. (2011). The era-interim reanalysis: Configuration and performance of the data assimilation system. *Quarterly Journal of the Royal Meteorological Society*, 137(656), 553–597. <https://doi.org/10.1002/qj.828>
- Donlon, C. J., Martin, M., Stark, J., Roberts-Jones, J., Fiedler, E., & Wimmer, W. (2012). The operational sea surface temperature and sea ice analysis (ostia) system. *Remote Sensing of Environment*, 116, 140–158.
- Emanuel, K. A., & Rotunno, R. (1989). Polar lows as arctic hurricanes. *Tellus A: Dynamic Meteorology and Oceanography*, 41(1), 1–17.
- Eyring, V., Bony, S., Meehl, G. A., Senior, C. A., Stevens, B., Stouffer, R. J., & Taylor, K. E. (2016). Overview of the Coupled Model Intercomparison Project Phase 6 (CMIP6) experimental design and organization. *Geoscientific Model Development*, 9(5), 1937–1958. <https://doi.org/10.5194/gmd-9-1937-2016>
- Føre, I., Kristjánsson, J. E., Kolstad, E. W., Bracegirdle, T. J., Sætra, Ø., & Røsting, B. (2012). A ‘hurricane-like’ polar low fuelled by sensible heat flux: High-resolution numerical simulations. *Quarterly Journal of the Royal Meteorological Society*, 138(666), 1308–1324. <https://doi.org/10.1002/qj.1876>
- Føre, I., Kristjánsson, J. E., Sætra, B., Røsting, B., & Shapiro, M. (2011). The full life cycle of a polar low over the Norwegian sea observed by three research aircraft flights. *Quarterly Journal of the Royal Meteorological Society*, 137(660), 1659–1673. <https://doi.org/10.1002/qj.825>
- Gervais, M., Shaman, J., & Kushnir, Y. (2018). Mechanisms governing the development of the north atlantic warming hole in the cesm-le future climate simulations. *Journal of Climate*, 31(15), 5927–5946.
- Gray, S. L., & Craig, G. C. (1998). A simple theoretical model for the intensification of tropical cyclones and polar lows. *Quarterly Journal of the Royal Meteorological Society*, 124(547), 919–947. <https://doi.org/10.1002/qj.49712454713>
- Greaker, M., & Rosendahl, K. E. (2017). *Petroleum activity in barents sea south-east - climate, economics and employment*. <https://www.klimasoksmal.no/wp-content/uploads/2019/10/Report-for-Greenpeace-og-NU-Petroleum-activity-BSE-Final.pdf>
- Haarsma, R. J., Roberts, M. J., Vidale, P. L., Senior, C. A., Bellucci, A., Bao, Q., et al. (2016). High Resolution Model Intercomparison Project (HighResMIP v1.0) for CMIP6. *Geoscientific Model Development*, 9(11), 4185–4208. <https://doi.org/10.5194/gmd-9-4185-2016>
- Harrold, T. W., & Browning, K. A. (1969). The polar low as a baroclinic disturbance. *Quarterly Journal of the Royal Meteorological Society*, 95(406), 710–723. <https://doi.org/10.1002/qj.49709540605>
- Hodges, K. I. (1994). A general method for tracking analysis and its application to meteorological data. *Monthly Weather Review*, 122(11), 2573–2586.
- Hodges, K. I. (1995). Feature tracking on the unit sphere. *Monthly Weather Review*, 123(12), 3458–3465.
- Hodges, K. I. (1999). Adaptive constraints for feature tracking. *Monthly Weather Review*, 127(6), 1362–1373.
- Hodges, K. I. (2008). Confidence intervals and significance tests for spherical data derived from feature tracking. *Monthly Weather Review*, 136(5), 1758–1777.
- Hoskins, B. J., & Valdes, P. J. (1990). On the existence of storm-tracks. *Journal of the Atmospheric Sciences*, 47(15), 1854–1864. [https://doi.org/10.1175/1520-0469\(1990\)047<1854:oteost>2.0.co;2](https://doi.org/10.1175/1520-0469(1990)047<1854:oteost>2.0.co;2)
- Huang, F., Zhou, X., & Wang, H. (2017). Arctic sea ice in cmip5 climate model projections and their seasonal variability. *Acta Oceanologica Sinica*, 36(8), 1–8.
- Jung, T., Gordon, N. D., Bauer, P., Bromwich, D. H., Chevallier, M., Day, J. J., et al. (2016). Advancing polar prediction capabilities on daily to seasonal time scales. *Bulletin of the American Meteorological Society*, 97(9), 1631–1647. <https://doi.org/10.1175/BAMS-D-14-00246.1>
- Kolstad, E. W. (2006). A new climatology of favourable conditions for reverse-shear polar lows. *Tellus A: Dynamic Meteorology and Oceanography*, 58.
- Kolstad, E. W., & Bracegirdle, T. J. (2008). Marine cold-air outbreaks in the future: An assessment of IPCC AR4 model results for the Northern Hemisphere. *Climate Dynamics*, 30(7–8), 871–885. <https://doi.org/10.1007/s00382-007-0331-0>
- Kolstad, E. W., Bracegirdle, T. J., & Zahn, M. (2016). Re-examining the roles of surface heat flux and latent heat release in a “hurricane-like” polar low over the barents sea. *Journal of Geophysical Research: Atmospheres*, 121(13), 7853–7867.
- Laffineur, T., Claud, C., Chaboureaud, J.-P., & Noer, G. (2014). Polar lows over the Nordic Seas: Improved representation in ERA-Interim compared to ERA-40 and the impact on downscaled simulations. *Monthly Weather Review*, 142(6), 2271–2289. <https://doi.org/10.1175/mwr-d-13-00171.1>

- Landgren, O. A., Batrak, Y., Haugen, J. E., Støylen, E., & Iversen, T. (2019). Polar low variability and future projections for the nordic and barents seas. *Quarterly Journal of the Royal Meteorological Society*, 145(724), 3116–3128.
- Mallet, P.-E., Claud, C., & Vicomte, M. (2017). North Atlantic polar lows and weather regimes: Do current links persist in a warmer climate? *Atmospheric Science Letters*, 18(8), 349–355. <https://doi.org/10.1002/asl.763>
- Mansfield, D. (1974). Polar lows: The development of baroclinic disturbances in cold air outbreaks. *Quarterly Journal of the Royal Meteorological Society*, 100(426), 541–554.
- Meyer, M., Polkova, I., Modali, K. R., Schaffer, L., Baehr, J., Olbrich, S., & Rautenhaus, M. (2021). Interactive 3-d visual analysis of era5 data: Improving diagnostic indices for marine cold air outbreaks and polar lows. *Weather and Climate Dynamics*, 2(3), 867–891.
- Michel, C., Terpstra, A., & Spengler, T. (2018). Polar mesoscale cyclone climatology for the nordic seas based on era-interim. *Journal of Climate*, 31(6), 2511–2532.
- Mizielinski, M. S., Roberts, M. J., Vidale, P. L., Schiemann, R., Demory, M.-E., Strachan, J., & Malcolm, A. (2014). High-resolution global climate modelling: The upscale project, a large-simulation campaign. *Geoscientific Model Development*, 7(4), 1629–1640. <https://doi.org/10.5194/gmd-7-1629-2014>
- Noer, G., & Lien, T. (2010). *Dates and positions of polar lows over the nordic seas between 2000 and 2010*. Norwegian Meteorological Institute Rep. https://www.met.no/publikasjoner/met-report/met-report-2010/_attachment/download/5e0da025-5d16-42a7-a273-79ad860a6119:13da-da8d9f3a71cd2c899b1b79f3b6e4bf81fe04/MET-report-16-2010.pdf
- Noer, G., Saetra, Ø., Lien, T., & Gusdal, Y. (2011). A climatological study of polar lows in the nordic seas. *Quarterly Journal of the Royal Meteorological Society*, 137(660), 1762–1772.
- Orimolade, A. P., Furevik, B. R., Noer, G., Gudmestad, O. T., & Samelson, R. M. (2016). Waves in polar lows. *Journal of Geophysical Research: Oceans*, 121(8), 6470–6481. <https://doi.org/10.1002/2016JC012086>
- Orimolade, A. P., Gudmestad, O. T., & Wold, L. E. (2017). Vessel stability in polar low situations. *Ships and Offshore Structures*, 12(sup1), S82–S87.
- Palma, D., Varnajot, A., Dalen, K., Basaran, I. K., Brunette, C., Bystrowska, M., et al. (2019). Cruising the marginal ice zone: Climate change and arctic tourism. *Polar Geography*, 42(4), 215–235. <https://doi.org/10.1080/1088937X.2019.1648585>
- Papritz, L., Rouges, E., Aemisegger, F., & Wernli, H. (2019). On the thermodynamic preconditioning of arctic air masses and the role of tropopause polar vortices for cold air outbreaks from fram strait. *Journal of Geophysical Research: Atmospheres*, 124(21), 11033–11050.
- Radovan, A., Crewell, S., Moster Knudsen, E., & Rinke, A. (2019). Environmental conditions for polar low formation and development over the nordic seas: Study of january cases based on the arctic system reanalysis. *Tellus A: Dynamic Meteorology and Oceanography*, 71(1), 1618131.
- Rasmussen, E. (1979). The polar low as an extratropical risk disturbance. *Quarterly Journal of the Royal Meteorological Society*, 105(445), 531–549. <https://doi.org/10.1002/qj.49710544504>
- Rasmussen, E., & Turner, J. (2003). *Polar lows: Mesoscale weather systems in the polar regions*. Cambridge University Press. https://link.springer.com/chapter/10.1007/978-1-878220-69-1_4
- Riahi, K., Rao, S., Krey, V., Cho, C., Chirkov, V., Fischer, G., et al. (2011). RCP 8.5—A scenario of comparatively high greenhouse gas emissions. *Climatic Change*, 109(1–2), 33–57. <https://doi.org/10.1007/s10584-011-0149-y>
- Rojo, M., Claud, C., Mallet, P.-E., Noer, G., Carleton, A. M., & Vicomte, M. (2015). Polar low tracks over the Nordic Seas: A 14-winter climatic analysis. *Tellus A: Dynamic Meteorology and Oceanography*, 67(1), 24660. <https://doi.org/10.3402/tellusa.v67.24660>
- Romero, R., & Emanuel, K. (2017). Climate change and hurricane-like extratropical cyclones: Projections for north atlantic polar lows and medicanes based on cmip5 models. *Journal of Climate*, 30(1), 279–299.
- Saha, S., Moorthi, S., Pan, H.-L., Wu, X., Wang, J., Nadiga, S., et al. (2010). The NCEP climate forecast system reanalysis. *Bulletin of the American Meteorological Society*, 91(8), 1015–1058. <https://doi.org/10.1175/2010bams3001.1>
- Smirnova, J., & Golubkin, P. (2017). Comparing polar lows in atmospheric reanalyses: Arctic system reanalysis versus era-interim. *Monthly Weather Review*, 145(6), 2375–2383.
- Smirnova, J. E., Zabolotskikh, E. V., Bobylev, L. P., & Chapron, B. (2016). Statistical characteristics of polar lows over the Nordic Seas based on satellite passive microwave data. *Izvestiya, Atmospheric and Oceanic Physics*, 52(9), 1128–1136. <https://doi.org/10.1134/s0001433816090255>
- Stoll, P. J., Graverson, R. G., Noer, G., & Hodges, K. (2018). An objective global climatology of polar lows based on reanalysis data. *Quarterly Journal of the Royal Meteorological Society*, 144(716), 2099–2117.
- Stoll, P. J., Spengler, T., Terpstra, A., & Graverson, R. G. (2021). Polar lows—moist-baroclinic cyclones developing in four different vertical wind shear environments. *Weather and Climate Dynamics*, 2(1), 19–36. <https://doi.org/10.5194/wcd-2-19-2021>
- Stroeve, J., Holland, M. M., Meier, W., Scambos, T., & Serreze, M. (2007). Arctic sea ice decline: Faster than forecast. *Geophysical Research Letters*, 34(9). <https://doi.org/10.1029/2007GL029703>
- Stroeve, J. C., Kattsov, V., Barrett, A., Serreze, M., Pavlova, T., Holland, M., & Meier, W. N. (2012). Trends in arctic sea ice extent from cmip5, cmip3 and observations. *Geophysical Research Letters*, 39(16).
- Terpstra, A., Michel, C., & Spengler, T. (2016). Forward and reverse shear environments during polar low genesis over the northeast atlantic. *Monthly Weather Review*, 144(4), 1341–1354.
- Terpstra, A., Renfrew, I. A., & Sergeev, D. E. (2021). Characteristics of cold-air outbreak events and associated polar mesoscale cyclogenesis over the North Atlantic region. *Journal of Climate*, 34(11), 4567–4584. <https://doi.org/10.1175/jcli-d-20-0595.1>
- Terpstra, A., Spengler, T., & Moore, R. W. (2015). Idealised simulations of polar low development in an Arctic moist-baroclinic environment. *Quarterly Journal of the Royal Meteorological Society*, 141(691), 1987–1996. <https://doi.org/10.1002/qj.2507>
- Terpstra, A., & Watanabe, S.-i. (2020). Polar lows. In *Oxford research encyclopedia of climate science*. <https://oxfordre.com/climatescience/view/10.1093/acrefore/9780190228620.001.0001/acrefore-9780190228620-e-775>
- Tous, M., Zappa, G., Romero, R., Shaffrey, L., & Vidale, P. L. (2016). Projected changes in medicanes in the HadGEM3 N512 high-resolution global climate model. *Climate Dynamics*, 47(5–6), 1913–1924. <https://doi.org/10.1007/s00382-015-2941-2>
- West, J. J., & Hovelsrud, G. K. (2010). Cross-scale adaptation challenges in the coastal fisheries: Findings from lebesby, northern Norway. *Arctic*, 338–354. <https://www.jstor.org/stable/20799601>
- Williams, K. D., Harris, C. M., Bodas-Salcedo, A., Camp, J., Comer, R. E., Copsey, D., et al. (2015). The met office global coupled model 2.0 (gc2) configuration. *Geoscientific Model Development*, 8(5), 1509–1524. <https://doi.org/10.5194/gmd-8-1509-2015>
- Woollings, T., Harvey, B., Zahn, M., & Shaffrey, L. (2012). On the role of the ocean in projected atmospheric stability changes in the atlantic polar low region. *Geophysical Research Letters*, 39(24).
- Xia, L., Zahn, M., Hodges, K. I., Feser, F., & von Storch, H. (2012). A comparison of two identification and tracking methods for polar lows. *Tellus A: Dynamic Meteorology and Oceanography*, 64(1), 17196. <https://doi.org/10.3402/tellusa.v64i0.17196>
- Yanase, W., Niino, H., Shun-ichi, I. W., Hodges, K., Zahn, M., Spengler, T., & Gurvich, I. A. (2016). Climatology of polar lows over the sea of Japan using the JRA-55 reanalysis. *Journal of Climate*, 29(2), 419–437. <https://doi.org/10.1175/jcli-d-15-0291.1>

- Zahn, M., & von Storch, H. (2008). A long-term climatology of North Atlantic polar lows. *Geophysical Research Letters*, 35(22). <https://doi.org/10.1029/2008gl035769>
- Zahn, M., & von Storch, H. (2010). Decreased frequency of north atlantic polar lows associated with future climate warming. *Nature*, 467(7313), 309–312. <https://doi.org/10.1038/nature09388>
- Zappa, G., Shaffrey, L., & Hodges, K. (2014). Can polar lows be objectively identified and tracked in the ecmwf operational analysis and the era-interim reanalysis? *Monthly Weather Review*, 142, 2596–2608.